ARTS AND SCIENCE
ARTS AND SCIENCE PRESS PTE. LTD

# Research Article

# Effect of Ti₃C₂-MXene size on cell viability of human carcinoma cells

Tianyi Dong[1], Ming Qi[1], Shuxia Ji[1], Kailin Liu[1], Peng Shi[1,*], Chong Geng[1,*]

[1] *Department of Breast and Thyroid Surgery, Shandong Provincial Hospital Affiliated to Shandong First Medical University, No. 324 Jingwu Road, Jinan 250021, Shandong Province, China.*

**\* Corresponding author:** Chong Geng, chonggeng_1982@163.com; Peng Shi, ship_slyy@163.com

## ABSTRACT

MXene nanoflakes, a new type of transition metal carbides, nitrides, and carbonitrides (named as MXene) have emerged as biocompatible transition metal structures, which illustrate desirable performance for various applications due to their unique physicochemical, and compositional virtues. MXenes are currently expanding their application from optical, chemical, electronic, and mechanical fields towards biomedical areas. In terms of biomedical applications, the biological toxicity of MXenes materials in different forms must be considered inevitably. In this paper, $Ti_3C_2$-MXene nanoflakes with different sizes have been prepared by means of wet etching method combined with powerful ultrasonication for exploring the effect in human breast carcinoma cells (MDA-MB-231 Cells) and human thyroid carcinoma cells (GLAG-66 Cells). Clinically representative MDA-MB-231 Cells and GLAG-66 Cells are selected as experimental subjects and their biotoxicities are characterized when exposed to $Ti_3C_2$-MXene nanoflakes with different sizes and concentrations. The results show that $Ti_3C_2$-MXene nanoflakes with sizes below 200 nm is almost non-toxic to MDA-MB-231 Cells and GLAG-66 Cells at low concentrations, and enhance their bioactivity and proliferation. When the nanoflake size is above 200 nm, $Ti_3C_2$-MXene has a significant inhibitory effect on the proliferation of the cells. This phenomenon may be due to the different roles of $Ti_3C_2$-MXene materials at different scales in cell proliferation as well as in complex physiological processes. This result is of great significance for material screening and design before biological experiments using $Ti_3C_2$-MXene.

*Keywords:* MXene; biological toxicity; human breast carcinoma cells；human thyroid carcinoma cells

## 1. Introduction

Cancer has become a leading factor threatening human health in recent years. Millions of death was caused by cancer every year worldwide with an increasing tendency. The rapid development in clinic biomedical and nanobiology have stimulated the creation of a variety of novel inorganic nano-systems that offers multiple theranostic modalities as potential alternatives to treating various diseases by synergistic therapy and multimodal imaging, especially in cancer theranostics. Currently, two-dimensional (2D) nanomaterials with ultrathin layered topological structure have been widely applied in biomedical multi-

disciplinary research[1-4]. These studies mainly include mostly explored graphene and its derivatives[5,6], hexagonal boron nitrides (h-BN)[7], transition metal dichalcogenides (TMDCs)[8], transition metal oxides (TMOs)[9], palladium (Pd) nanosheets [10,] black phosphorus (BP)[11], and transition metal carbides (MXenes)[12]. The high specific surface areas and promising physical and chemical properties enable them to meet the stringent requirements of nanotherapeutic drugs, such as drug delivery, phototherapy, diagnostic imaging, biosensors, and even tissue engineering [13-15].

MXenes are a kind of novel multifunctional 2D nanomaterials developed by Barsoum, which contains large amounts of transition metal carbides, nitrides, and carbonitrides with metallic conductivity and hydrophilic nature as well as excellent mechanical properties[14]. MXenes are usually fabricated by the selective extraction of A-element from layered ternary carbides of $M_{n+1}AX_n$ (MAX) phases (n = 1–3), where M is an early transition metal (e.g., Ti, Mo, Zr, V, Ta or Nb), A is the terminated with surface moieties, such as a mixture of –OH, =O, and –F, and X is C and/or N [16-19]. MXenes typically have three kinds of formulas: $M_2X$, $M_3X_2$, and $M_4X_3$[20]. The high specific surface areas of MXenes nanoflakes make them as potential drug or protein carriers with rich anchoring sites and reservoirs [21]. In addition, the controllable composition and tunable in-plane structure of MXenes can be precisely designed and synthesized within the original structure of the MAX phases, which makes a flexible and broad range of multifunctional MXenes suitable for promising therapeutic nanomedicine. To date, MXenes with a variety of different traction physicochemical properties and biological effects have attracted increasing attention [22].

Recently, the vitro studies on cytotoxicity of MXenes has been investigated. Anita et al. explored the effect of surface charge of MXenes on its antibacterial function [23]. Błażej et al. compared and summarized the cytotoxicity of MXenes to human fibroblasts and cervical cancer cells [24]. Jastrzębska et al. studied the rapid in situ oxidation of 2D V2CTz MXene in culture cell media and their cytotoxicity as well as the cytotoxicity of $Ti_3C_2$ (MXene) flakes exposed to cancerous and benign cells by post-delamination surface modifications [25, 26]. The sizes of MXene flakes will bring the change of physical and chemical properties, thus trigger different physiological processes, however, the vitro cytotoxicity of MXenes flakes with different sizes has not been addressed, which makes the application possibilities and health risks unaware.

In this work, for exploring the $Ti_3C_2$-MXene flakes with different sizes applicatins in MDA-MB-231 Cells and GLAG-66 Cells, the highly quality $Ti_3C_2$-MXene flakes are prepared by wet etching method combined with powerful ultrasonication. Firstly, the characterics of the prepared $Ti_3C_2$-MXene flakes are characterized by different means. Such as, The surface morphologies with the different resolution are investigated by scanning electron microscope (SEM) and Transmission electron microscope (TEM). The structural properties before and after preparation of $Ti_3C_2$-MXene are characterized by X-ray diffraction (XRD) and X-ray photoelectron spectroscopy (XPS), respectively.Subsequently, based on the parpared the $Ti_3C_2$-MXene flakes, the exploratory experiments were carried out. By exposing the clinically representative human breast carcinoma cells and human thyroid carcinoma cells to the well-dispersed $Ti_3C_2$-MXene flakes with different lateral sizes and concentrations, the biotoxicities of the cells are evaluated. The cytotoxicity of $Ti_3C_2$-MXene flakes with different sizes on the MDA-MB-231 cells and GLAG-66 cells are analyzed and compared. The acquired results could provide valuable basis for the $Ti_3C_2$-MXene applications in adjacent biomedical field.

## 2. Results and discussion

### 2.1. Synthesis and characterization of Ti$_3$C$_2$-MXene flakes

The highly dispersed suspension of ultrathin Ti$_3$C$_2$-MXene flakes is synthesized by delaminating a Ti$_3$AlC$_2$ precursor with hydrofluoric acid (HF) by selectively etching its Al layers under certain circumstances. (the detailed preparation process of the Ti$_3$C$_2$-MXene flakes are given in the Methods Section). **Figure 1** shows the properties of MXene nanomaterials in different states characterized by SEM. **Figure1(a)** shows the Ti$_3$AlC$_2$ precursor particles. **Figure 1 (b)** illustrates the loosely stacked structure of the etched Ti$_3$C$_2$ particles. Since the well-exfoliated Ti$_3$C$_2$-MXene flakes are ultrathin and nearly transparent, the clean surface and edges are observed as shown in Figure 1 (c). Subsquently, the Ti$_3$C$_2$-MXene flakes with large sizes are crushed into smaller nanoflakes using powerful ultrasonication, and three representative sizes of about 5 nm, 200 nm and above 500 nm are obtained. **Figure 2** shows the characteristics of prepared nanoflakes with different sizes at different resolution by TEM.
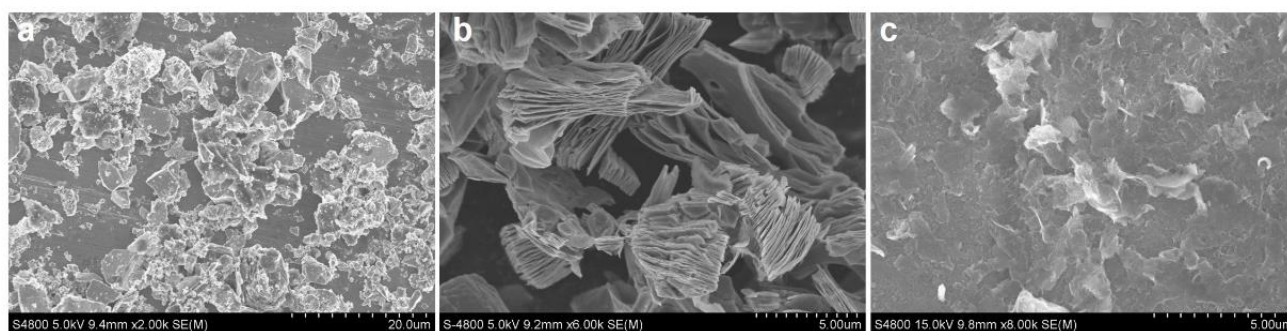


**Figure 1.** SEM images of (a) Ti$_3$AlC$_2$ precursor particle, (b) Ti$_3$C$_2$ particle obtained after etching, (c) Dispersed Ti$_3$C$_2$ flakes.
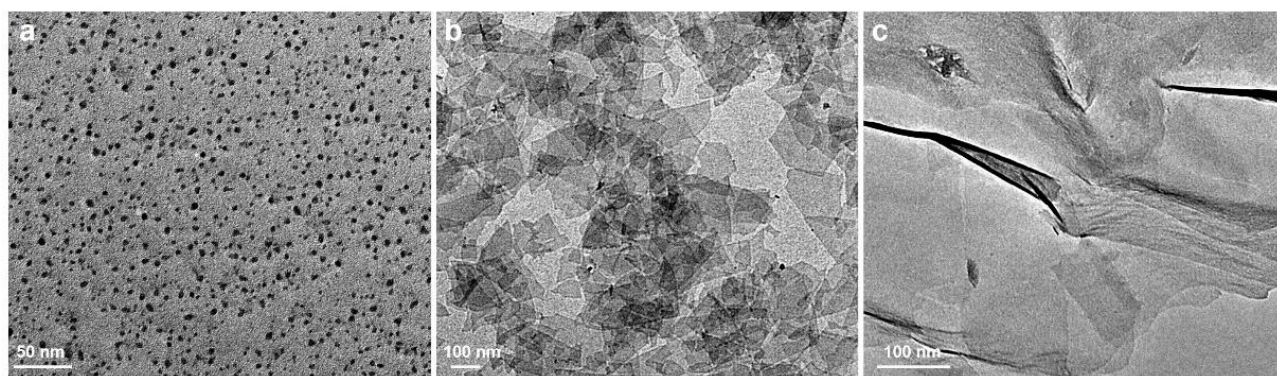


**Figure 2.** TEM images of as-prepared flakes fabricated by powerful ultrasonication after HF etching, with three representative sizes (a) about 5 nm, (b) about 200 nm, (c) above 500 nm.

The detailed structural properties of the nanoflakes materials were further determined by the XRD pattern as shown in **Figure 3 (a)** indicates the successful synthesis of Ti$_3$C$_2$-MXene phase. As can be seen in this figure, the peak intensities originating from the parent Ti$_3$AlC$_2$ bulk decrease substantially after HF etching treatment. The lower peak shift of the basal planes occurs because of the removal of Al in the Ti$_3$AlC$_2$ and the presence of F and OH functional groups. And the XPS measurements of Ti$_3$AlC$_2$ phase after HF etching treatment (Ti$_3$C$_2$-MXene flakes) are performed to identify the elemental compositions. From the XPS survey scan spectrum shown in **Figure 3 (b)**, the F and O groups are also detected in the as-prepared Ti$_3$C$_2$-MXene flakes besides Ti and C groups. The exi stence of F and O groups implies that the surfaces of the Ti$_3$C$_2$-MXene flakes are mostly terminated with F, OH and/or O groups, which is also found in previous research [27, 28].
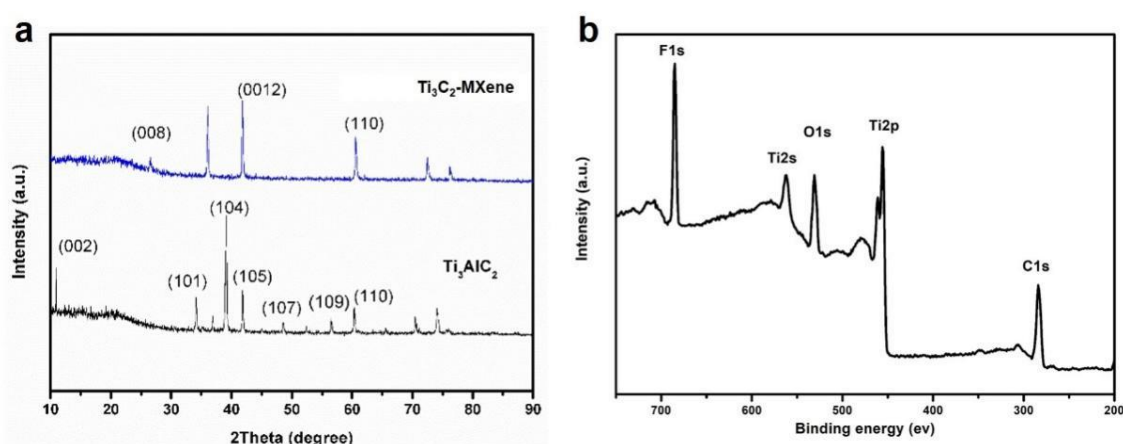
3

**Figure 3 (a).** XRD patterns of $Ti_3AlC_2$ before and after HF etching treatment ($Ti_3C_2$-MXene).(b) Typically XPS results of $Ti_3C_2$-MXene flakes.

## 2.2. Cell proliferation evaluation

To evaluate the effect of $Ti_3C_2$-MXene flakes sizes on cell viability of human carcinoma cells, clinically representative MDA-MB-231 Cells and GLAG-66 cells are used as experimental subjects. The sizes of $Ti_3C_2$-MXene flakes are around 5 nm, 200 nm and above 500 nm, respectively. After exposing the cells into the $Ti_3C_2$-MXene flakes for 24 hours, the viability of both MDA-MB-231 cells and GLAG-66 cells exhibit a concentration-dependent reduction with the $Ti_3C_2$-MXene flakes concentration increased from 0 to 500 μg/mL, as shown in **Figure 4** and **5**. Compared with the control cells, as the concentration of $Ti_3C_2$-MXene flakes increases from 25 to 50 μg/mL, the cell viability is significantly decreased. However, when the concentration is above 50 μg/mL, different sizes of $Ti_3C_2$-MXene flakes have almost no effect on cell viability. For the $Ti_3C_2$-MXene flakes with sizes at about 200 nm and above 500 nm, the viabilities of MDA-MB-231 cells and GLAG-66 cells obviously begin to decrease when the concentration increases above 5 μg/mL. The results indicate that the size of the $Ti_3C_2$-MXene flakes have significant effect on the cell viability. The reason why $Ti_3C_2$-MXene flakes of the size at 200 nm and above 500 nm begin to inhibit cell viability at relatively low concentration may be attributed that larger sizes tend to cause more damage to cell membrane. The $Ti_3C_2$-MXene flakes with three different sizes show no cell specificity, indicating that they are probably effective on more types of cancer cells.
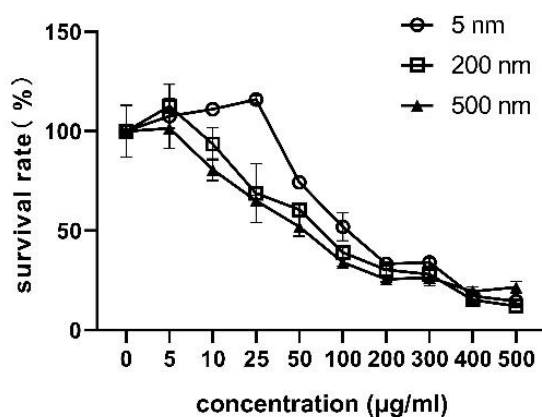


**Figure 4.** Relative viabilities of MDA-MB-231 cells after being incubated with varied concentrations (0, 5, 10, 25, 50, 100, 200, 300, 400, 500 μg/ml) of $Ti_3C_2$-MXene flakes. Error bars are based on the standard deviations of three parallel samples with the flakes of 5 nm, 200 nm, 500 nm.
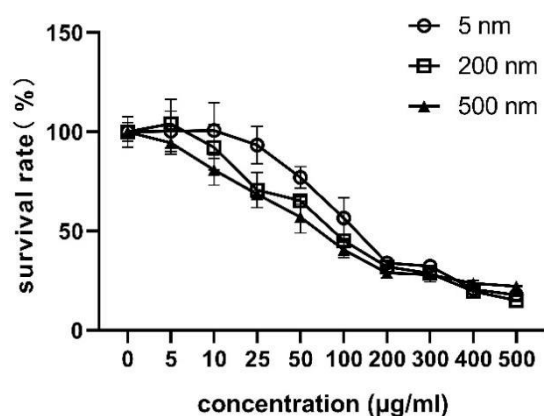
4

**Figure 5.** Relative viabilities of GLAG-66 Cells after being incubated with varied concentrations (0, 5, 10, 25, 50, 100, 200, 300, 400, 500 µg/ml) of $Ti_3C_2$-MXene flakes. Error bars are based on the standard deviations of three parallel samples with the flakes of 5 nm, 200 nm, 500 nm.

## 3. Materials and methods

### 3.1. Preparation of $Ti_3C_2$-MXene flakes

**Figure 6** shows the detailed preparation process. The $Ti_3AlC_2$ (1 g) powder (Nanjing Mission new Materials Co. Ltd.) is added into the hydrofluoric (HF) acid solution (40 wt%) over the course of 10 min, and immersed in an ice bath to avoid overheating. The reaction mixture is kept at 40 °C for 48 h while stirring vigorously, after which the mixture is repeatedly washed with deionized water until the supernatant is almost neutral pH ($\geq 6$). To obtain stable colloid MXene flakes, the washed mixture is subsequently sonicated with an ultrasound probe (700 W) for 1 h. The volumetric bottle is cooled to 10 °C by circulating water, and the ultrasonic instrument is set in 5 s/1 s working/intermittent mode, which can avoid the high temperature-induced additional damage to the structure. The final colloid is obtained by removing the bottom sediment and left for 3 months without significant changes.
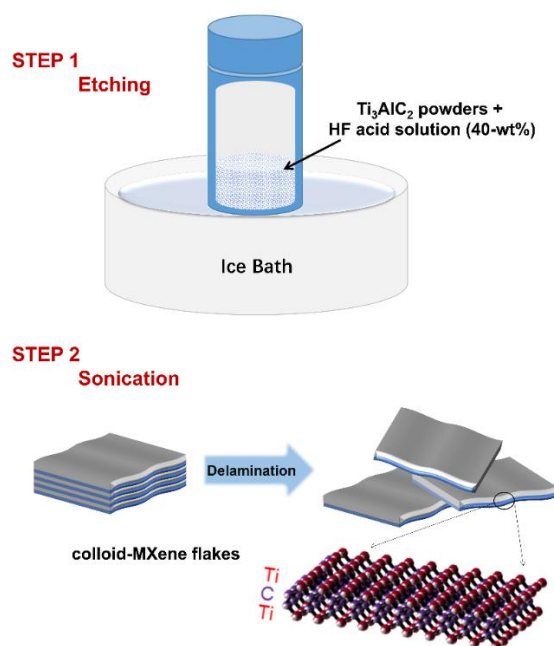


**Figure 6.** Schematic of synthesis of $Ti_3C_2$-Mxene flakes.

### 3.2. Characterization of $Ti_3C_2$-MXene flakes

The morphology and structure of the obtained $Ti_3C_2$-MXene flakes are observed by scanning electron microscopy (HITACHI S-4800). The fine structure of the obtained $Ti_3C_2$-MXene flakes is characterized by JEM-2100F high resolution transmission electron microscopy (JEOL, Akishima-shi, Japan) operated at 200 kV. The XRD patterns of the $Ti_3C_2$-MXene powder are recorded by Bruker-AXS D8 Advance X-ray diffractometer with Cu K$\alpha$ irradiation ($\lambda$ = 1.5406 Å). The XPS patterns of the $Ti_3C_2$-MXene flakes are recorded by spectrometer (Thermo Fisher Scientific Escalab 250) equipped with an Al K$\alpha$ source, where C 1s (284.6 eV) is used to calibrate the peak positions of various elements.

### 3.3. Cell culture

MDA-MB-231 cells and GLAG-66 cells are cultured in Dulbecco's Modified Eagle Medium (DMEM) (Thermo Scientific, Waltham, MA, USA) supplemented with 10% heat-inactivated fetal bovine serum (Thermo Scientific, Waltham, MA, USA), 100 units/mL penicillin, 100 μg/mL streptomycin (Thermo Scientific, Waltham, MA, USA), and 2 mM l-glutamine (Thermo Scientific, Waltham, MA, USA) at 37°C in a humidified atmosphere of 5% $CO_2$ and 95% air.

### 3.4. Treatment and CCK-8 assay

Cells are trypsinized, counted, seeded in 96-well plate ($5 \times 10^3$ cells/well) and serum-starved for 24 hours before treatment. Cells are stimulated for 24 hours with different concentrations (0, 5, 10, 25, 50, 100, 200, 300, 400, 500 μg/ml) of $Ti_3C_2$-MXene flakes. Cells are incubated with CCK8 (10 μl/well, Dojindo, Kumamoto, Japan) for 2 h and the optical density values are then measured by using a spectrophotometer with 450 nm optical source.

## 4. Discussion

Cancer is a leading cause of death and projected to be the most important barrier to increasing life expectancy in every country of the world. Cancer ranks as the first or second leading cause of death before the age of 70 in most countries according to World Health Organization (WHO) estimates. There were 19.3 million new cases of cancer and almost 10 million deaths from cancer in 2020 according to GLOBOCAN data (GLOBOCAN 2020) [29]. Cancer incidence and mortality are rapidly growing due to increased life expectancy and lifestyle changes that increase cancer risk. Surgery and radiotherapy are the main modalities for non-metastatic cancers, anti-cancer drugs (chemotherapy, biological therapies) are the therapeutic options currently used in metastatic cancers. Chemotherapy is based on the suppression of the division of rapidly growing cells which is a characteristic of malignant cells or slow their growth, however, it also affects non-cancer cells with fast rates of replication, such as the bone marrow hematopoietic stem cells, digestive tract mucosa, skin and its appendages cells, producing the characteristic side effects of chemotherapy. The destruction of normal cells, the toxicity of conventional chemotherapeutic agents, together with the development of multi-drug resistance, encourage the need to explore new effective treatments based on novel therapeutic targets of the tumor cells[30, 31].

Nanotechnology has exhibited high-certainty biomedical applications in the field of drug discovery and delivery [32-34]. Previous studies have already found that extremely sharp edges of graphene nanosheets could result in damage of bacterial membrane integrity, such sharp edges can induce membrane stress on bacteria by acting as cutters [35]. The mechanism of "cutting cells" may be exploited to develop novel potential anti-cancer therapeutic agents. On the basis of this study, we believe that there will be more research work on MXene in clinical oncology to explore more in-depth and detailed mechanism and provide rich clinical validation data.

# 5. Conclusions

Ti$_3$C$_2$-MXene flakes with different sizes have been prepared by means of wet etching method combined with powerful ultrasonication. TEM results show that the distinct lateral-size distributions of Ti$_3$C$_2$-MXene flakes are about 5 nm, 200 nm and above 500 nm, respectively. XRD and XPS results suggest that the structure and composition of Ti$_3$C$_2$-MXene flakes are preserved well. The cytotoxicity of Ti$_3$C$_2$-MXene flakes towards human breast carcinoma cells and human thyroid carcinoma cells is characterized, which shows that Ti$_3$C$_2$-MXene flakes with larger size exhibit stronger cytotoxicity activity than that of smaller ones. In addition, the Ti$_3$C$_2$-MXene flakes also display different concentration-dependent cytotoxicity activity. The Ti$_3$C$_2$-MXene flakes with large size strongly influence the cell proliferation activity at relatively low concentration (<10 µg/mL). The size-dependent cell cytotoxicity of Ti$_3$C$_2$-MXene flakes may come from their different aggregation states or oxidation capacity. Ti$_3$C$_2$-MXene flakes with larger size are easier to cover cells, which can block their active sites on membranes. Cells cannot proliferate once fully covered, resulting in the cell viability loss in the counting test. In contrast, Ti$_3$C$_2$-MXene flacks with smaller size can adhere to the cell surfaces or enter the cell, which cannot effectively isolate cells from environment, thus result in the weaker cytotoxicity. This study highlights the importance of tailoring the lateral dimension of Ti$_3$C$_2$-MXene flakes to optimize the potential application for clinical health and safety with minimal risks.

# Author contributions

Chong Geng and Peng Shi designed and developed the whole project and wrote the manuscript. Tianyi Dong and Ming Qi performed sample processing and helped data analysis. Shuxia Ji and Kailin Liu provided technical support in cell culture. All authors have read and agreed to the published version of the manuscript.

# Funding

# Institutional Review Board Statement

Not applicable.

# Informed Consent Statement

Not applicable.

# Data Availability Statement

Not applicable.

# Conflicts of Interest

The authors declare no conflict of interest.

# References

1. Xing, Z.; Chang, Y.; Kang, I. Immobilization of biomolecules on the surface of inorganic nanoparticles for biomedical applications. Sci. Technol. Adv. Mater. 2010, 11, 014101.
2. Juan, L.; Vivero, E.; Huang, Y. Inorganic-Organic Hybrid Nanomaterials for Therapeutic and Diagnostic Imaging Applications. Int. J. Mol. Sci. 2011, 12, 3888-3927.
3. Hong Liu, Huazhang Guo, Yibin Fang, Liang Wang, and Peng Li, Rational Design of Nitrogen-Doped Carbon Dots for Inhibiting b-Amyloid Aggregation, Molecules, 2022, 28, 1451.

4.  Weitao Li , Luoman Zhang, Ningjia Jiang, Yongqian Chen, Jie Gao, Jihang Zhang, Baoshuo Yang, and Jialin Liu, Fabrication of Orange Fluorescent Boron-Doped Graphene Quantum Dots for Al3+ Ion Detection, Molecules, 2022, 27, 6771.

5.  Joanna, J.; Adrian, C.; Magdalena, B.; Marcin, G.; Ludwika, L. Synthesis and Characterization of Graphene Oxide and Reduced Graphene Oxide Composites with Inorganic Nanoparticles for Biomedical Applications. Nanomater. 2020, 10, 1846.

6.  Govindasamy, R.; Zhang, X.; Thandapani, G.; Wang, S.; Mohammad, A.; Govindarasu, M.; Gnanasundaram, N.; Mohammad, A.; Ill-Min, C. Current Use of Carbon-Based Materials for Biomedical Applications—A Prospective and Review. Processes 2020, 8, 355.

7.  Faiz, U. S.; Sergei, G.; Oleg, N. A. Boron in Tribology: From Borates to Ionic Liquids. Tribol. Lett. 2013, 51, 281–301.

8.  Fan, Y.; Sun, W. J.; Shi. X. Y. Design and Biomedical Applications of Poly (amidoamine)-Dendrimer-Based Hybrid Nanoarchitectures. Small Methods 2017, 11, 1700220.

9.  Jalal, A.; Parshant, K.; Vijay, K. S.; Zdenek, S. Surface Functionalization of 2D Transition Metal Oxides and Dichalcogenides via Covalent and Non-covalent Bonding for Sustainable Energy and Biomedical Applications. ACS Appl. Nano Mater. 2020, 3, 3116–3143.

10. Abdulhadee, Y.; Chanika, P.; Weena, S.; Orawon. C. Biomedical Probes Based on Inorganic Nanoparticles for Electrochemical and Optical Spectroscopy Applications. Sensors 2015, 15, 21427-21477.

11. Qian, X. Q.; Gu, Z.; Chen. Y.; Two-dimensional black phosphorus nanosheets for theranostic nanomedicine. Mater. Horiz. 2017, 4, 800-816.

12. Zhang, H.; Liu, J.; Tian, Z.; Ye, Y.; Cai, Y.; Liang, C.; Kazuya, T. A general strategy toward transition metal carbide/carbon core/shell nanospheres and their application for supercapacitor electrode. Carbon 2016, 100, 590-599.

13. Vogel, A.; Noack, J.; Hüttman, G.; Paltauf, G. Mechanisms of femtosecond laser nanosurgery of cells and tissues. Appl. Phys. B 2005, 81, 1015–1047.

14. Juliette, S.; Emmanuel, F.; Muriel, G. Overview of carbon nanotubes for biomedical applications. Materials 2019, 12, 624.

15. Neves, V.; Heister, E.; Costa, S.; Tîlmaciu, C.; Flahaut, E.; Soula, B.; Coley, H.M.; McFadden, J.; Silva, S.R.P. Design of double-walled carbon nanotubes for biomedical applications. Nanotechnology 2012, 23, 365102.

16. Faisal Shahzad, Mohamed Alhabeb, Christine B. Hatter, Babak Anasori, Soon Man Hong, Chong Min Koo, Yury Gogotsi, Electromagnetic interference shielding with 2D transition metal carbides (MXenes). Science, 2016, 353, 1137-1140.

17. Yongchang Dong, Sergii Chertopalov, Kathleen Maleski, Babak Anasori, Longyu Hu, Sriparna Bhattacharya, Apparao M. Rao, Yury Gogotsi, Vadym N. Mochalin, and Ramakrishna Podila, Advanced Materials, 2018, 30 1705714.

18. Feng Pan, Shuang Wang, Zhipeng Yong, Xiaodong Wang, Chenglong Li, Dan Liang, Xiaorui Wang, Han Sun, Yinghe Cui and Zhe Wang, An All-Solid-State Flexible Supercapacitor Based on MXene/MSA Ionogel and Polyaniline Electrode with Wide Temperature Range, High Stability, and High Energy Density, Molecules, 2023, 28, 1554.

19. Yasuaki, O.; Natha, K.; James, M.; Goff; Shin'ichi, H.; Kosuke, H.; Ismaila, N. MXene Electrode Materials for Electrochemical Energy Storage: First-Principles and Grand Canonical Monte Carlo Simulations. MRS Advances 2019, 4, 1833–1841.

20. Michael, N.; Vadym, N. M.; Michel, W. B.; Yury, G. 25th Anniversary Article: MXenes: A New Family of Two-Dimensional Materials. Adv. Mater. 2014, 26, 992-1005.

21. Shahzad, F.; Iqbal, A.; Kim, H.; Koo, C. M. 2D Transition Metal Carbides (MXenes): Applications as an Electrically Conducting Material. Adv. Mater. 2020, 32, 2002159.

22. Persson; POA; Rosen, J. Current state of the art on tailoring the MXene composition, structure, and surface chemistry. Curr. Opin. Solid St. M. 2019, 23, 100774.

23. Anita, R.; Joanna, M.; Aleksandra, S.; Michał, C.; Jarosław, W.; Mateusz, P.; Tomasz, W.; Alexey, S. V.; Agnieszka, M. J. Engineering of 2D $Ti_3C_2$ MXene Surface Charge and its Influence on Biological Properties. Materials 2020, 13, 2347.

24. Błażej, S.; Jacek, K. W.; Magdalena, S.; Barbara, P.; Marcin, J.; Grzegorz, N.; Łucja, P. Cytotoxicity Assessment of Ti–Al–C Based MAX Phases and $Ti_3C_2Tx$ MXenes on Human Fibroblasts and Cervical Cancer Cells. ACS Biomater. Sci. Eng. 2019, 5, 6557–6569.

25. Jastrzębska, A. M.; Scheibe, B.; Szuplewska, A.; Rozmysłowska-Wojciechowska, A.; Chudy, M.; Aparicio, C.; Scheibe, M.; Janica, I.; Ciesielski, A.; Otyepka, M.; Barsoum, M. W. On the rapid in situ oxidation of two-dimensional V2CTz MXene in culture cell media and their cytotoxicity. Mater. Sci. Eng. C 2021, 119, 111431.

26. Jastrzębska, A. M.; Szuplewska, A.; Rozmysłowska-Wojciechowska, A.; Chudy, M.; Olszyna, A.; Birowska, M.; Popielski, M.; Majewski, J. A.; Scheibe, B.; Natu, V.; Barsoum, M. W. On tuning the cytotoxicity of $Ti_3C_2$

(MXene) flakes to cancerous and benign cells by post-delamination surface modifications. 2D Mater. 2020, 7, 025018.

27. Xue, Q.; Zhang, H. J.; Zhu, M. S.; Pei, Z. X.; Li, H. F.; Wang, Z. F.; Huang, Y.; Huang, Y.; Deng, Q. H.; Zhou, J.; Du, S. Y.; Huang, Q.; Zhi, C. Y. Photoluminescent $Ti_3C_2$ MXene Quantum Dots for Multicolor Cellular Imaging. Adv. Mater. 2017, 29, 1604847.

28. Wu, Q.; Li, N. B.; Wang, Y.; Xu, Y.C.; Wu, J. D.; Jia, G. R.; Ji, F. J.; Fang, X. D.; Chen, F. F.; Cui, X. Q. Ultrasensitive and Selective Determination of Carcinoembryonic Antigen Using Multifunctional Ultrathin Amino-Functionalized $Ti_3C_2$ MXene Nanosheets. Anal. Chem. 2020, 92, 3354.

29. Hyuna Sung, Jacques Ferlay, Rebecca L Siegel, Mathieu Laversanne, Isabelle Soerjomataram, Ahmedin Jemal, Freddie Bray, Global Cancer Statistics 2020: GLOBOCAN Estimates of Incidence and Mortality Worldwide for 36 Cancers in 185 Countries, CA Cancer J Clin, 2021, 71, 209-249.

30. Tiantian Tan, Jie Li, Ruhua Luo, Rongrong Wang, Liyan Yin, Mengmeng Liu, Yiying Zeng, Zhaowu Zeng, Tian Xie, Recent Advances in Understanding the Mechanisms of Elemene in Reversing Drug Resistance in Tumor Cells: A Review, Molecules, 2021, 24, 5792.

31. Edgar Pérez-Herrero, Alberto Fernández-Medarde, Advanced targeted therapies in cancer: Drug nanocarriers, the future of chemotherapy, Eur J Pharm Biopharm, 2015, 93, 52-79.

32. Chen-Yang Zhao, Rui Cheng, Zhe Yang, Zhong-Min Tian, Nanotechnology for Cancer Therapy Based on Chemotherapy, Molecules, 2018, 23, 826.

33. Lianjie Ye, Larwubah Kollie, Xing Liu, Wei Guo, Xiangxian Ying, Jun Zhu, Shengjie Yang, Meilan Yu, Antitumor Activity and Potential Mechanism of Novel Fullerene Derivative Nanoparticles, Molecules, 2021, 26, 3252.

34. Luisa Sonntag, Juliane Simmchen, Veronika Magdanz, Nano-and Micromotors Designed for Cancer Therapy, Molecules, 2019, 24, 3410.

35. Omid Akhavan 1, Elham Ghaderi, Toxicity of graphene and graphene oxide nanowalls against bacteria, ACS nano, 2010, 4, 5731.